MICROHETEROGENEITY IN ULTRA-HIGH STRENGTH LOW ALLOY STEEL AFTER THREE REGIMES OF HEAT-TREATMENT

J. DOBROVSKÁ[1)], V. DOBROVSKÁ[1)], J. POKLUDA[2)], K. STRÁNSKÝ[2)], D. MANDRINO[3)] AND M. JENKO[3)]

[1)] *Technical University of Ostrava, Ostrava, Czech Republic*
[2)] *Brno University of Technology, Brno, Czech Republic*
[3)] *Institute of Metals and Technology, Ljubljana, Slovenia*

ABSTRACT

The chemical microheterogeneity in three differently heat treated samples of the ultra-high low alloy steel was measured by means of an original method based on the space concentration distribution of 9 alloying and impurity elements. Additionally, the high resolution Auger electron spectroscopy was applied in order to analyse directly the presence of alloying elements at grain boundaries. By combination of results achieved by both experimental methods, the different fracture behaviour of investigated steel grades is explained on the bases of a dissimilar distribution of Mo, C and P at grain boundaries.

KEYWORDS

Chemical microheterogeneity, high strength steel, grain boundary segregation, intergranular fracture, fracture toughness, absorbed energy, Auger spectroscopy.

EXPERIMENTAL METHODS AND SAMPLES

The aim of the paper was to analyse the chemical microheterogeneity of elements and their presence at prior austenite grain boundaries in differently heat treated samples of ultra-high strength low alloy steel of various grain size and dissimilar fracture behaviour. Results of this analysis were expected to be useful for the qualitative interpretation of fracture mechanisms and morphologies.

Determination of the chemical microheterogeneity of elements was performed by means of the original method published in [1-3]. Principles and application of this method are following:

- The concentration of elements is measured in regular equi-distant sites on the selected section of a metallographic sample. Usually, a segment of 300 μm length is analysed, containing a total number of 101 measured sites (3 μm distant).
- As a measuring device, the point quantitative energy dispersion X-ray microanalysis was used equipped by a special software package and measuring device connected with the *JXA 8600/KEVEX Delta V Sezame* analytical complex.

- After finishing the concentration measurement, the surface of the metallographic sample was etched in order to visualise the contamination of the surface caused by electron beam and, consequently, the measured sites were photographically documented.
- The database of measured concentration of elements is corrected by means of the ZAF correction system (Z – atomic number, A- absorption, F – fluorescent intensification).
- Statistical analysis of the corrected concentration data of each element enables us to obtain: (i) index of chemical heterogeneity of the element I_H , (ii) the effective distribution coefficient in the matrix structure k_{ef} and (iii) correlation coefficients k_{ij} between elements in the structural segment.

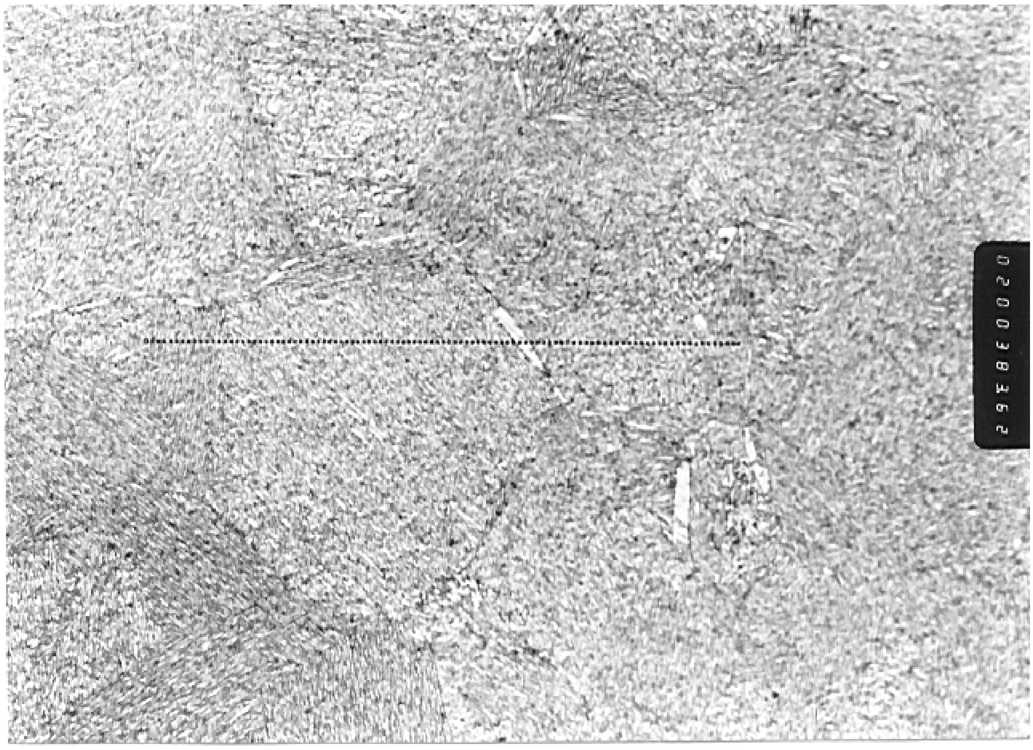

Fig. 1. Example of concentration measuring on the coarse-grained sample 7(S3). Etched by *nital 2%* after the measurement (magnification 200x).

Analysis of the presence of elements at prior austenite grain boundaries was performed by means of the high-resolution Auger electron spectroscopy (HRAES). This method is based on the precise measurement of the kinetic energy of Auger electrons emitted from atoms as a consequence of a special rearrangement of their electronic structure [4]. Each atom exhibits its characteristic Auger spectrum. The VG-Scientific Microlab 310-F used in these experiments is equipped by a spherical sector analyser and the field emission gun producing an electron beam of 10 nm in diameter. An ultra-high vacuum stage was used in order to obtain fresh fracture surfaces of metallic samples.

The experimental procedure started by introducing notch cylindrical specimens of analysed steel grades into the chamber of the Microlab 310-F. The samples were colded to –120 ^{o}C and fractured *in situ* in ultra high vacuum and the fresh fracture surfaces were analysed by means of the HRAES.

The chemical composition of the PLDHA steel of the Czech provenience is in tab. 1. The microstructure of the material samples corresponded to a low- or middle tempered martensite.

Table 1. Chemical composition of ultra-high strength low alloy PLDHA steel [wt.%]

C	Mn	Si	P	S	Cr	Ni	Mo	V
0.40 - 0.44	0.65 - 0.85	1.50 - 1.80	max 0.015	max 0.010	0.70 - 0.90	1.60 - 1.90	0.30 - 0.50	0.05 - 0.10

The heterogeneity of following elements was analysed: silicon, phosphorus, vanadium, chromium, manganese, iron, nickel, molybdenum and carbon. Carbon concentration within the measured segment was expressed by means of the spectral line intensity C$K\alpha$ in imp./s. An example of the measured structural segment on the metallographic sample is shown in Fig. 1.

Characteristics of applied heat treatments, corresponding structures and prevalent fracture surface morphology is presented in tab. 2.

Table 2. Three regimes of the heat treatment, grain structure and fracture morphologies [5]

Sample	Solution annealing and quenching ^{o}C/h/	Tempering ^{o}C/h/	Microstructure	Fracture morphology
3(S1)	870/1/oil	300/2/air	fine-grained standard	transgranular – ductile dimple
5(D3)	1200/1.5/oil	480/1.5/oil	coarse-grained degraded	intergranular – ductile dimple
7(S3)	1200/1.5/oil	300/2/air	coarse-grained – standard	intergranular – brittle decohesion

Absorbed energy and fracture toughness K_{Ic} related to different heat treatments are presented in tab. 3.

Table 3. Impact absorbed energy and fracture toughness [5]

Sample	Absorbed energy [J]		Fracture toughness K_{Ic} [MPa.m$^{1/2}$]
	Charpy U-notch	Charpy V-notch	-
3(S1)	48.7	38.1	51.0
5(D3)	12.5	-	83.0
7(S3)	12.3	-	79.0

EXPERIMENTAL RESULTS

Parameters of the chemical heterogenity of elements are shown in tab. 4 and 5. Tab. 4 includes measured and calculated values of the mean concentration of elements in selected segments c_{mean}, indices of heterogeneity I_H and their effective distribution coefficients k_{ef}. Index of heterogeneity is defined as the ratio of the standard deviation s_x of the element concentration and its arithmetic average c_{mean} measured along the particular segment, i.e. $I_H = s_x / c_{mean}$. Effective distribution coefficient k_{ef} contents information about the original liquation of elements during crystallisation between the solid and liquid phases. The way of its determination is a part of the original software package. Tab. 5 includes the coefficients of pair correlation of all the analysed elements with respect to iron.

Table 4. Parameters of chemical heterogeneity of elements in the samples

Sample	Parameter	Element [wt.]					Carbon [imp/s]			
		Si	P	V	Cr.	Mn	Fe	Ni	Mo	C
3(S1)	c_{mean}	1.4008	0.0488	0.112	1.057	0.458	94.07	2.153	0.693	101.19
	I_H	0.0613	0.4584	0.324	0.092	0.209	0.005	0.096	0.490	0.1104
	c_{hef}	0.9481	0.6725	0.750	0.924	0.835	1.004	0.953	0.711	0.9091
5(D3)	c_{mean}	1.3815	0.0422	0.116	1.057	0.449	94.04	2.169	0.744	107.38
	I_H	0.0596	0.5586	0.333	0.074	0.214	0.003	0.087	0.110	0.1102
	k_{ef}	0,9530	0.6145	0,747	0.941	0.832	1.003	0.925	0.903	0.9106
7(S3)	c_{mean}	1.4180	0.0410	0.122	1.093	0.480	93.83	2.224	0.792	111.34
	I_H	0.0447	0.5493	0.301	0.074	0.218	0.003	0.091	0.127	0.1030
	k_{ef}	0.9620	0.6215	0.768	0.935	0.828	1.003	0.923	0.896	0.9130

Table 5. Coefficients of pair correlation k_{XFe} (X = Si, P, V, Cr, Mn, Fe, Ni, Mo and C)

Sample	Si	P	V	Cr	Mn	Fe	Ni	Mo	C
3(S1)	-0.403	-0.018	-0.318	-0.280	-0.180	1.000	-0.473	-0.797	0.000
5(D3)	-0.306	-0.166	-0.133	-0.357	-0.452	1.000	-0.781	-0.414	0.102
7(S3)	-0,365	-0.064	-0.016	-0.042	-0.505	1.000	-0.774	-0.423	0.045

Difference between individual samples comes particularly to the fore when ordering elements according to the decreasing sequence of I_H as shown in tab. 6.

Table 6. Sequences of elements - decreasing heterogeneity index

Sample	1	2	3	4	5	6	7	8	9
3(S1)	Mo	P	V	Mn	C	Cr	Ni	Si	Fe
5(D3)	P	V	Mn	Ni	Cr	C	Mo	Si	Fe
7(S3)	P	V	Mn	Mo	Ni	C	Cr	Si	Fe

From those results, the following conclusions can be summarised:

- Distribution of all the analysed elements in the sample 3(S1) – the fine grained standard – is heterogeneous. The index of heterogeneity I_H decreases with the following sequence of elements: Mo, P, V, Mn, C, Ni, Cr, Si a Fe from the value $I_H = 0.490$ (for Mo) to the value $I_H = 0.005$ (for Fe).
- Due to the solution annealing at the temperature 1200 °C with the duration of 1.5 hour, the chemical heterogeneity in samples 5(D3) a 7(S3) becomes substantially lower.
- Index of heterogeneity of elements in the sample 5(D3) solution annealed for coarse grain and tempered for grain boundary embrittlement decreases with the following sequence of elements: P, V, Mn, Ni, Cr, C, Mo, Si and Fe from the value $I_H = 0.559$ (for P) to the value $I_H = 0.003$ (for Fe).
- Index of heterogeneity of elements in the sample 7(S3), solution annealed for coarse grain but standardly tempered, decreases with the following sequence of elements: P, V, Mn, Mo, Ni, C, Cr, Si a Fe from the value $I_H = 0.549$ (for P) to the value $I_H = 0.003$ (for Fe).
- Coarsening of grains due to the high temperature solution annealing is assisted by the increase in heterogeneity of P unlike to all other analysed elements.
- The significant decrease in the heterogenity of Mo in coarse grained samples when compared to the fine grained 3(S1) specimen is extremely important (I_H = 0,110 resp. 0,127 vs. I_H = 0,490 - see tab. 4).
- Interstitial carbon has slightly higher heterogeneity in the 5(D3) than in the 7(S3) sample.

The X-ray microanalysis of heterogeneity can yield only indirect and relative information about the concentrations of elements at grain boundaries. However, a higher concentration of P and a lower concentration of Mo can be expected in coarse grained samples.

The HRAES analysis yielded following generalised results concerning the presence of selected elements at prior austenite grain boundaries:

- In the standard sample 3(S1) only negligible traces of alloying elements were found bounded in fine carbides or sulphides. Carbon was distributed in the solid solution as well as in fine carbides within the dimples (see Fig. 2).
- In the sample 7(S3) individual large complex sulphides were found containing Mo, Ti , Ni or Cr (P1 in Fig. 3). Carbon was distributed in both the solid solution (P2 and P3 in Fig. 3) and small carbides within the dimples (P4 and P5 in Fig. 3).
- In the sample 5(D3) traces of alloying elements were found bounded in smaller sulphides (P1 and P4 in Fig. 4) or carbides (P1 in Fig. 5). Carbon was predominantly concentrated

in carbides situated in dimples even at grain boundary facets (see Fig. 5). Its concentration in the solid solution was very low in comparison to both the samples 3(S1) and 7(S3) – see P3 and P4 in Fig. 4 or P2 and P3 in Fig. 5.

DISCUSSION OF RESULTS

The following questions are to be clarified on the bases of experimental analyses:

(i) What is the reason of intergranular fracture of samples 5(D3) and 7(S3) and the related decrease in the impact toughness as well as increase in the fracture toughness.

(ii) Why the 5(D3) specimen exhibits prevalently a dimple intergranular morphology whereas the morphology of the 7(S3) specimen was predominantly an intergranular decohesion.

The first question can be answered by the different behaviour of Mo and P in coarse grained 5(D3) and 7(S3) samples in comparison to the fine grained standard 3(S1). In coarse grained structures, the heterogeneity of phosphorus significantly increased whereas the heterogeneity of molybdenum decreased. It means that a number of Mo atoms (protecting against the grain boundary embrittlement) left their positions at grain boundaries and surrendered them to severe P atoms. This process has led to the intergranular fracture mode possibly supported by the stress concentration effect at the front of dislocation pile-ups in the coarse grains. Consequently, a significant decrease in the impact toughness was observed in case of 5(D3) and 7(S3) samples in comparison with the 3(S1) sample. The increase in fracture toughness can be explained by the high level of crack tip shielding induced by the tortuous intergranular crack front in 5(D3) and 7(S3) samples [5,6]. This effect reduces the crack driving force in comparison to that of the straight transgranular crack in the 3(S1) sample and, therefore, the fracture toughness of 5(D3) and 7(S3) samples was higher.

The second problem can be solved when joining the results of both the HRAES and X-ray analyses:

- In the sample 5(DS3) treated for the temper embrittlement, carbon and other alloying elements are concentrated in carbide and sulphur precipitates at grain boundaries and the adjacent matrix zone remains depleted. The related lack of substitution hardening enhances the plasticity in the surrounding of carbides. It leads to the nucleation and growth of shallow ductile dimples within the thin depleted zone along grain boundaries and, consequently, to the intergranular dimple fracture morphology in spite of a higher segregation of the phosphorus.
- Both the lower concentration of carbides at grain boundaries and the absence of the ductile grain boundary zone exclude the dimple fracture mechanisms in the sample 7(S3). Therefore, an intergranular decohesion supported by segregation of phosphorus was the preferential fracture mode in this case.
- In the fine grained sample 3(S1), the lower concentration of segregated phosphorus and the higher grain boundary area lead to a lower surface activity of the phosphorus. Simultaneously, the higher concentration of molybdenum retards the tendency to the intergranular fracture. All those factors favour the transgranular dimple fracture mode.

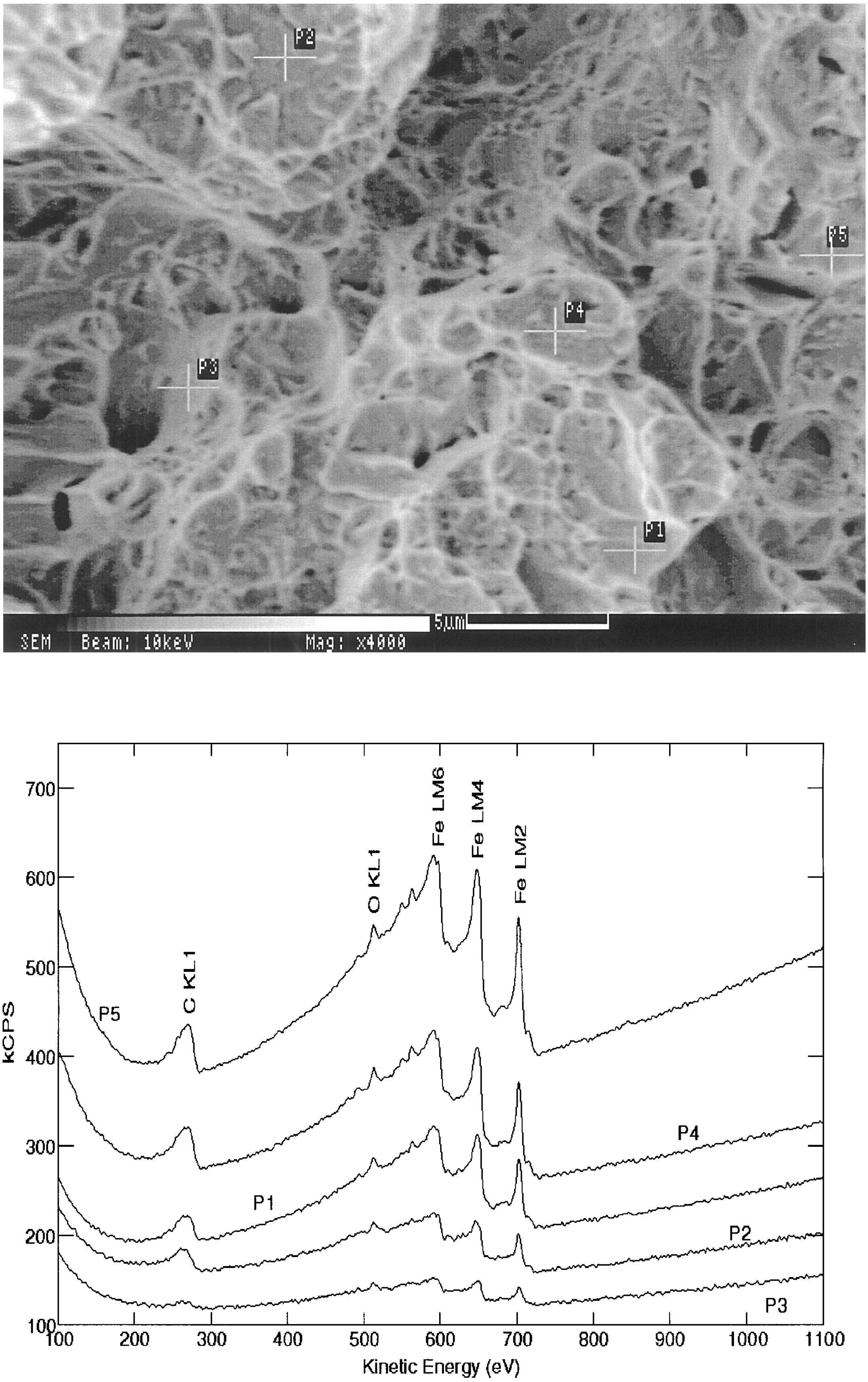

Fig. 2. Auger spectra from the fracture surface of the sample 3(S1).

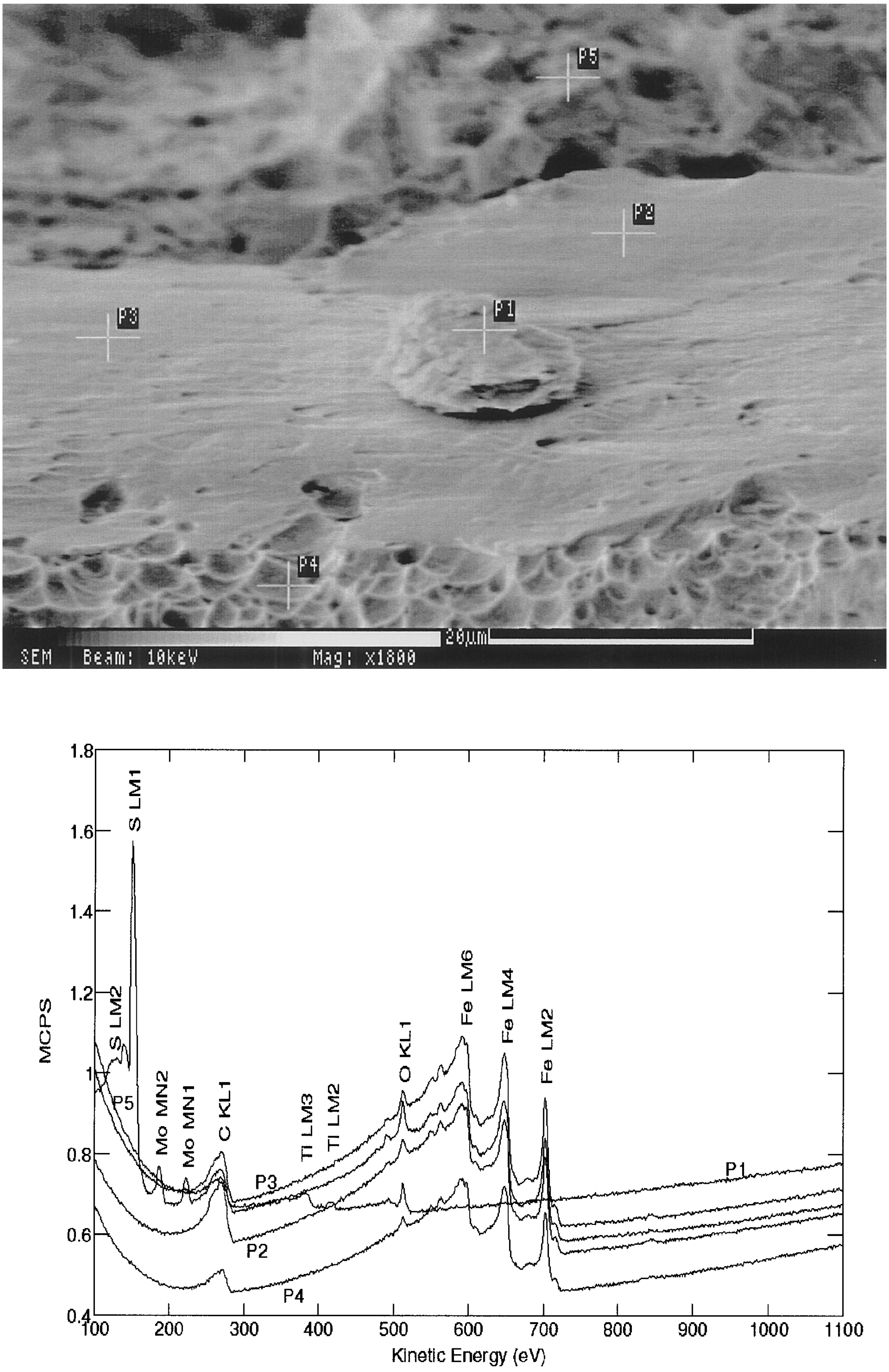

Fig. 3. Auger spectra from the fracture surface of the sample 7(S3).

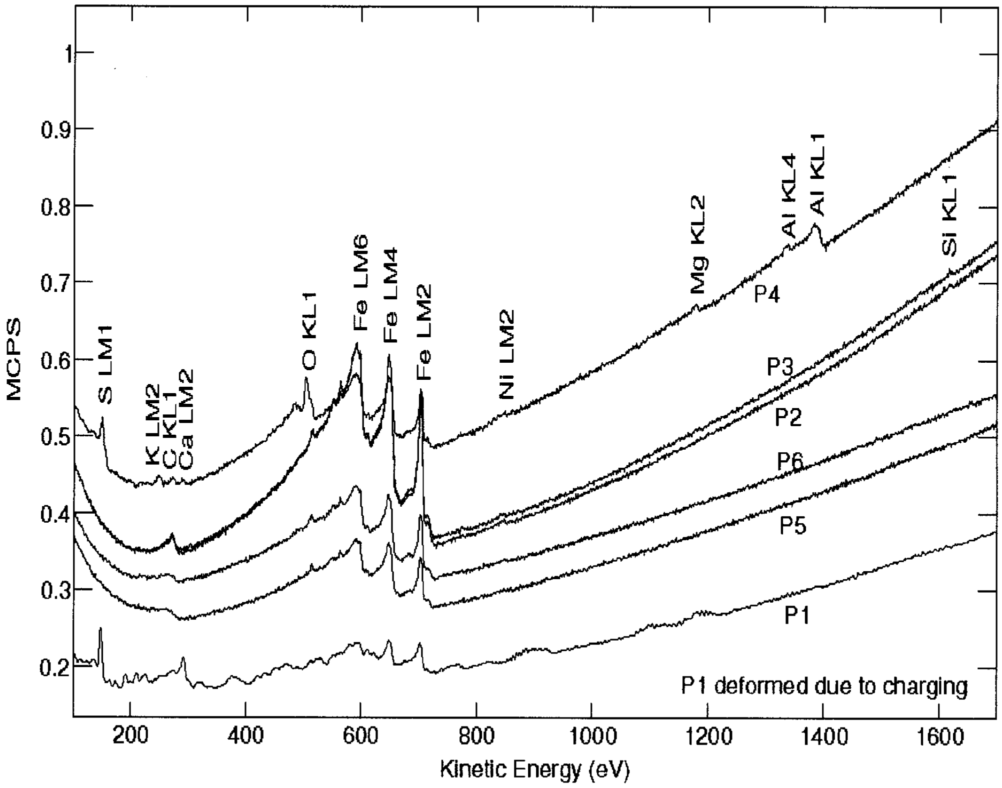

Fig. 4. Auger spectra from the fracture surface of the sample 5(D3).

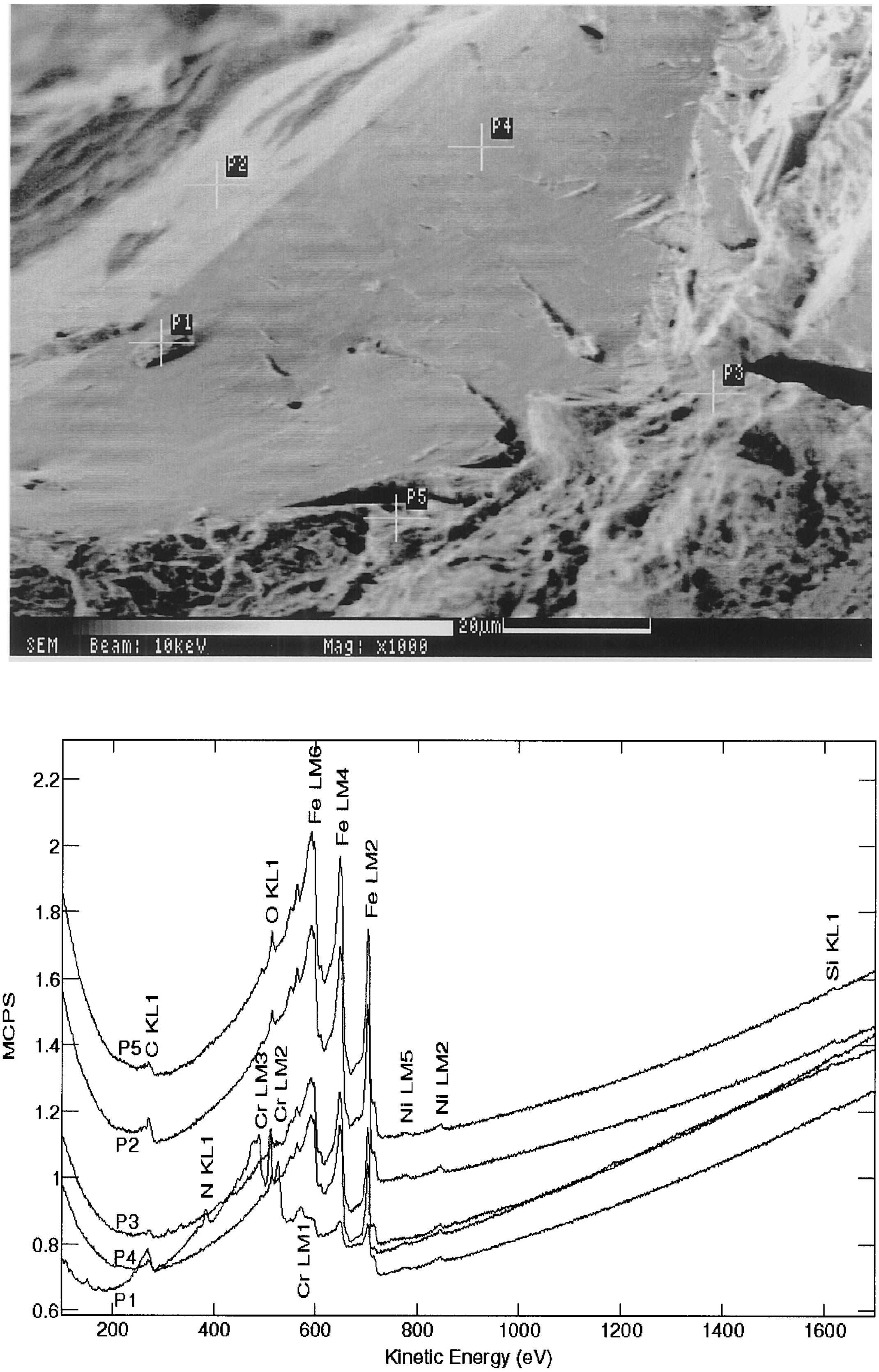

Fig. 5. Auger spectra from the fracture surface of the sample 5(D3).

CONCLUSION

Application of two different experimental methods based on X-ray and Auger spectrometry enabled a qualitative elucidation of different fracture behaviour of three grades of the ultra-high strength low alloy steel. The intergranular fracture in coarse grained samples was induced by the enhanced segregation of phosphorus and migration of Mo atoms from boundaries to the grain interior. The shallow ductile dimples at intergranular facets of the specimen tempered for the grain boundary embrittlement appeared as a consequence of a thin ductile zone along grain boundaries depleted of carbon and other alloying elements. This zone has created due to the extreme precipitation of complex carbides and sulphides at grain boundaries.

ACKNOWLEDGEMENT

This work was supported by the European agency COST (Action 517), the Ministry of Education and Youth of the Czech Republic under the Grant No. OC 517.30 (1998), the Ministry of Education, Science and Sport of Republic of Slovenia, No. RP 0206-503

REFERENCES

[1] Dobrovská V., Dobrovská J., Rek A. and Stránský K.: Kovové Mater. 33, (1995), 8 (in Czech).
[2] Dobrovská V., Dobrovská J., Rek A. and Stránský K.: Kovové Mater. 33, (1995), 462 (in Czech).
[3] Dobrovská V., Dobrovská J., Rek A. and Stránský K.: Scripta Mater. 38, (1998), 1583.
[4] Jenko M, Fine J. and Mandrino D.: Surf Interface Anal 30 (2000) 350.
[5] Pokluda J., Šandera P., Vlach B., Jurášek L.: In: Cleaner Metals for Industrial Exploitation, Int. Workshop, Action 517 COST (in press).
[6] Pokluda J., Šandera P. and Zeman J.: Amer. Soc. Test. Mater. – Spec. Techn. Publication 1131, 1992, 653.